Energy 36 (2011) 3791–3803

Contents lists available at ScienceDirect

Energy

journal homepage: www.elsevier.com/locate/energy

Proposal and analysis of a dual-purpose system integrating a chemically recuperated gas turbine cycle with thermal seawater desalination

Chending Luo [a,b,*], Na Zhang [a], Noam Lior [c], Hu Lin [a,b]

[a] Institute of Engineering Thermophysics, Chinese Academy of Sciences, PO Box 2706, Beijing 100190, PR China
[b] Graduate School of the Chinese Academy of Sciences, PO Box 2706, Beijing 100190, PR China
[c] Department of Mechanical Engineering and Applied Mechanics, University of Pennsylvania, Philadelphia, PA 19104-6315, USA

ARTICLE INFO

Article history:
Received 28 February 2010
Received in revised form
5 October 2010
Accepted 17 November 2010
Available online 12 January 2011

Keywords:
Chemically recuperated gas turbine (CRGT)
MED-TVC
Seawater desalination
Power and water cogeneration
Dual purpose plants

ABSTRACT

A novel cogeneration system is proposed for power generation and seawater desalination. It combines the CRGT (chemically recuperated gas turbine) with the MED-TVC (multi-effect thermal vapor compression desalination) system. The CRGT contains a MSR (methane-steam reformer). The produced syngas includes plenty of steam and hydrogen, so the working medium flow increases and NO_x emissions can achieve 1 ppm low. However, the water consumption is large, ~23 t/d water per MW power output. To solve this problem and produce water for sale, MED-TVC is introduced, driven by exhaust heat. Such a dual-purpose plant was analyzed to investigate its performance and parameter selection, and compared with four conventional cogeneration systems with the same methane input. Some main results are following: In the base case of the CRGT with a TIT of 1308 °C and a compression ratio of 15, the MED-TVC with 9 effects, the specific work output, performance ratio and CRGT-consumed water ratio are 491.5 kJ/kg, 11.3 and 18.2%, respectively. Compared with the backpressure ST (steam turbine)/CC (combined cycle) plus MED/MSF (multistage flash), the CRGT + MED has better thermal performance, lower product cost and shorter payback period, which indicates the CRGT + MED dual-purpose system is a feasible and attractive choice for power and water cogeneration.
© 2010 Elsevier Ltd. All rights reserved.

1. Introduction

CRGT (Chemically recuperated gas turbine) cycles combine a natural gas fired gas-turbine cycle with a chemical recuperation process [1–6]. In such cycles turbine exhaust heat is recovered in a HRSG (heat recovery steam generator) and the superheater is replaced by a MSR (methane steam reformer) to produce syngas, in which the following reactions occur [7,8]:

$$CH_4 + H_2O \leftrightarrow CO + 3H_2 \quad \Delta H = 206.11\text{kJ} / (\text{mol } CH_4)$$

$$CO + H_2O \leftrightarrow CO_2 + H_2 \quad \Delta H = -41.17\text{kJ} / (\text{mol CO})$$

$$C_nH_m + nH_2O \leftrightarrow nCO + (m/2 + n)H_2$$

The exhaust heat is thus recuperated chemically by the methane conversion to H_2 and CO. Comparing the syngas to the methane, the fuel heating value is raised [9]. It shows that low pressure, high temperature and high steam consumption help to increase the reforming conversion rate (the ratio between the converted methane to the methane input) [10]. Even though the fuel conversion is based on the available gas turbine exhaust and reaches only a moderate level, the basic chemically recuperated cycle (without inter-cooling or reheat) simulated by Kesser [2] still achieved a thermal efficiency of 48.8%, higher than that of the STIG (steam injected gas turbine). Owe to the presence of a significant amount of steam and hydrogen in the reformed gas, the NO_x emissions has been estimated to be as low as 1 ppm [2] and the specific power output becomes higher than that of a dry gas turbine cycle [11]. Such a cycle also has, however, large water consumption, about 23 t/d water per MW power output, which restricts the application of the plant; especially in water-short areas [2]. A preliminary economic evaluation of the CRGT system [7] indicated that it is economically feasible only if a low-cost source of water is available. However, compared to the CC (Combined Cycle, composed of a gas-turbine cycle and a steam turbine cycle, usually having a thermal efficiency of 51–58%), the little lower thermal efficiency, much simpler configuration (an MSR instead of an entire steam turbine cycle configuration) and ultra low NO_x emissions still make CRGT quite attractive.

Seawater desalination is widely used commercially to produce fresh water [12]. LT-MED (Low temperature multi-effect desalination) is one of the commonly used heat-driven desalination methods [13–24]. MED systems often have 4 to 12 effects. For example, in

* Corresponding author. Graduate School of the Chinese Academy of Sciences, PO Box 2706, Beijing 100190, PR China. Tel.: +86 10 82543030; fax: +86 10 82543019.
E-mail address: lcd866@hotmail.com (C. Luo).

0360-5442/$ – see front matter © 2010 Elsevier Ltd. All rights reserved.
doi:10.1016/j.energy.2010.11.029

Nomenclature

A	Total heat transfer area [m^2]
a	Specific heat transfer area [m^2/(kg/s)]
C	Cost [k$]
CR	Concentration ratio
COE	Cost of electricity [$/kWh]
COW	Cost of water [$/t]
E	Exergy [kW]
e	Specific exergy [kW/kg]
H	Annual running hours [h]
h	Enthalpy [kJ/kg]
i	Discount rate
m	Mass flow [kg/s]
n	Number of the effects or plant life [y]
PBP	Payback period [y]
PR	Performance ratio
Q	Thermal energy [kW]
R	Annual revenue of the plant [k$]
R_{NC}	Methane conversion rate
R_{pw}	Power-to-water ratio
R_{SN}	Steam-NG mole ratio
T	Temperature [K]
t	Temperature [°C]
TBT	Top brine temperature [°C]
TIT	Turbine inlet temperature [°C]
TPC	Total plant cost [k$]
U	Heat-transfer coefficient
W	Work [kW]
x	Steam-air mass ratio
β	Annual average investment coefficient
π	Compression ratio
ε	Exergy efficiency
η	Thermal efficiency
η_{isn}	Isentropic efficiency
δ	CRGT-consumed water ratio
ΔT_p	Minimum heat transfer temperature difference [°C]
ΔT_{eq}	Chemical equilibrium approach temperature difference [°C]

Subscripts

0	Base cycle
a	Ambient state
b	Boiler
air	Inlet air of the CRGT cycle
C	Condenser
cm	Condensate of the motive steam
COM	Compressor
con	Consumption
E	Evaporator
en	Entrained steam
ex	Exhaust gas
f	Flue gas
fu	Fuel
h	Heating steam
in	Input
m	Motive steam
net	Net value
om	Operation and maintenance
P	Pump
PHE	Preheater
pow	Power subcycle
s	Inlet steam of the MSR
syn	Syngas
T	Turbine
w	Water production
w,tol	Total water produced by MED

Ref. [14], two MED operating modes (parallel and parallel/cross) were studied, with the parallel/cross flow system having the better performance. Although the *TBT* (top brine temperature) in MED system is lower than 70 °C, the motive steam is often with a pressure around 3 bar (~134 °C) extracted from steam turbines or ranging from 20 to 30 bar (212–234 °C) supplied directly from a boiler [15,16]. From the second law of thermodynamics viewpoint, the big temperature difference causes much exergy loss in the heat exchange process, so the TVC (thermal vapor compressor) is introduced to improve the system thermal performance: the motive steam firstly entrains and compresses a fraction of the vapor produced in an effect of the MED, and then the mixture discharges as the heating steam at a temperature of about 70 °C [17,18].

Compared with the MED plant without vapor compression, such a MED-TVC arrangement meets the desalination temperature requirements better and achieves a higher performance ratio *PR*, which is defined as the ratio between the mass flow rates of the produced fresh water m_w to that of the consumed motive steam m_m,

$$PR = m_w/m_m \tag{1}$$

Meanwhile, the needs of cooling water and pumping power are also decreased [13].

In a MED with mechanical vapor compression system, the MVC (mechanical vapor compressor) can improve the performance of the MED as well as the TVC, but the TVC is adopted in this paper rather than the MVC for its effectiveness, easier operation and maintenance, and good economic characteristics [19].

Integration of the CRGT plant with a MED-TVC desalination system allows it to be supplied with its needed fresh water without depending on other water supplies. In this cogeneration system, the low temperature motive steam for driving the MED-TVC is generated by the CRGT turbine exhaust heat recovery that avoids a great waste of exergy if such low-grade thermal energy were provided directly by burning fuel in a boiler. It's obvious that the synergy of the power and water dual-purpose plants has significant energy, economy and environment benefits [12,13,20].

The main objective of this paper is to propose and analyze an integrated cogeneration system composed of a CRGT (as the prime mover) and a MED-TVC (as the bottom cycle). To investigate the performance and parameter selection of the energy, exergy and water production of the integrated cycle, the cogeneration system was modeled, analyzed and compared to some typical conventional power and water cogeneration systems with the same input. An economic perspective was held to evaluate the costs of electricity and fresh water and the payback periods of the different dual-purpose plants. A parametric sensitivity analysis was also performed to examine the influence of three important parameters, the steam-air mass flow rate ratio x of the CRGT, the saturation temperature of the motive steam t_m and the number of MED effects n. The results were discussed to further clarify the synergy of the integrated system.

2. The cogeneration system configuration

The flow sheet of the cogeneration system is given in Fig. 1a and b. As shown in Fig. 1a, the key process of the CRGT cycle is the reforming

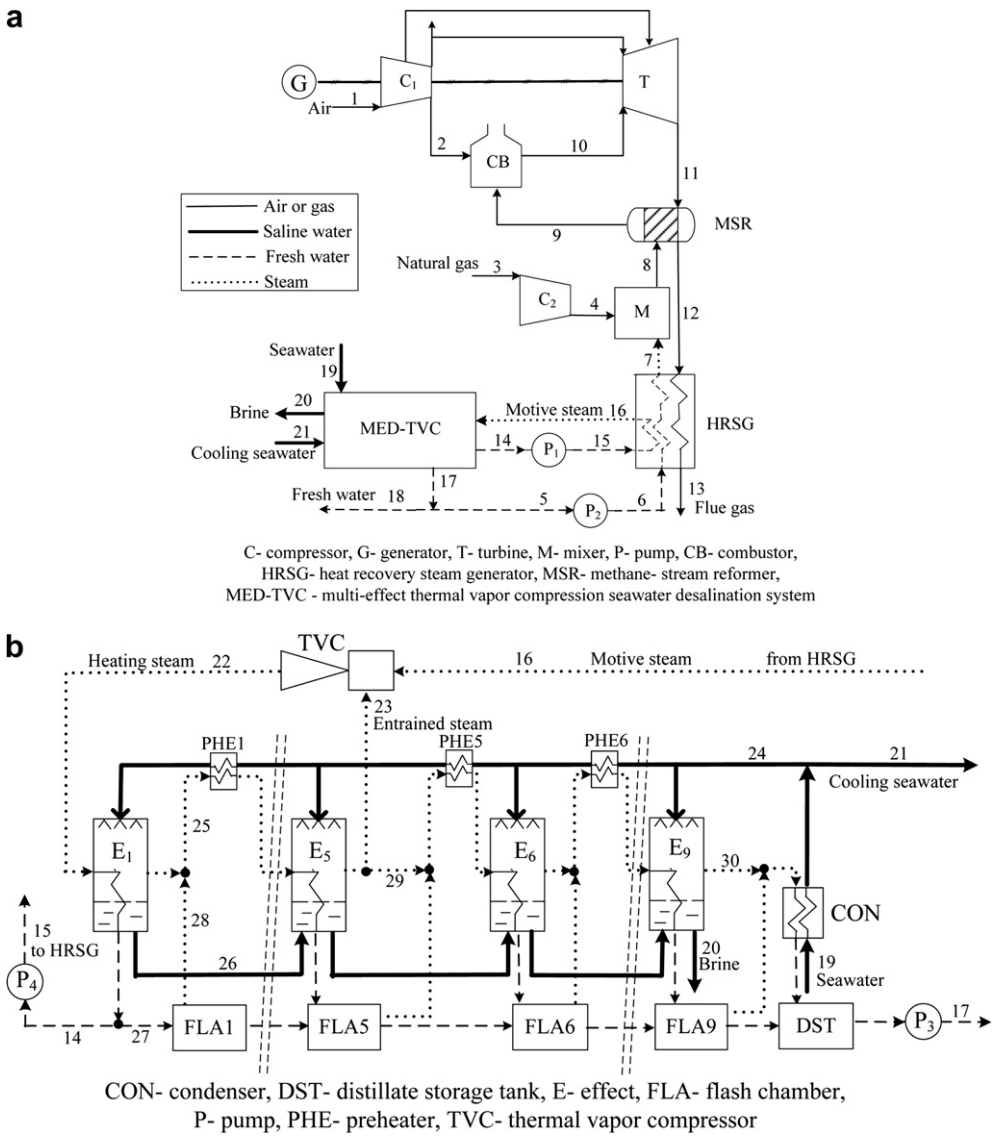

Fig. 1. a. Flow sheet of the CRGT+MED dual-purpose system, b. Flow sheet of the MED-TVC section in the dual-purpose system.

between the superheated steam and compressed NG (natural gas) in the MSR, which represents recovering of the turbine exhaust heat both thermally and chemically. The integration of the CRGT and MED-TVC is embodied in the motive steam (16) generation in the HRSG and the fresh water (6) supply to the CRGT. The extracted saturated steam (16) is sent into the TVC to run the MED-TVC bottom cycle.

Fig. 1b illustrated the MED-TVC system. The seawater is fed into the nine effects in parallel.

Using the TVC (thermal vapor compressor), the motive steam (16) compresses a part (23) of the vapor generated in the effect 5 (E5), at a medium temperature. In the TVC the expansion of the motive steam compresses the entrained vapor, and their mixture is discharged from the TVC and used as the heating steam (22) for the distillation process. It is thereby condensed and provides heat for seawater evaporation in the first effect (E1).

Part of the condensate (14) is returned into the HRSG, and the remainder (27) is introduced into flash chamber 1 (FLA1), where a small amount of vapor (28) flashes off because of a pressure drop. The vapor (25) evaporated from the seawater in E1 is mixed with the vapor (28) and the mixture vapor passes through the PHE1 (preheater 1) before routed into E2 (effect 2) to serve as the heat source together with the brine from E1 (26). The condensate of the vapor flows into FLA2 (flash chamber 2).

This process is repeated in all effects except for E5 and E9. In E5, part of the vapor is entrained by the TVC (23) (research shows that entraining vapor from an intermediate effect is better than from the last effect for enhancing the performance ratio *PR* [21]; only the remainder (29) is introduced into the PHE5 (preheater 5). While in E9, the vapor (30) is sent into the end CON (condenser) to preheat the seawater (19) before it flows into the DST. Part of the preheated seawater is used as the feed of the nine effects (24), and the balance (21) is rejected back to the sea, and so is the brine (concentrated seawater) outflow from E9 (20).

3. The cogeneration system simulation

3.1. Computation model and assumptions

Some properties of the feed steams are reported in Table 1. The proposed systems have all been modeled with the ASPEN PLUS software [25], in which the component simulation is based on energy, mass and species balances, with the default relative convergence

Table 1
Composition and some properties of feed streams.

	Natural gas	Air	Seawater
CH_4 (mol%)	100	–	–
N_2 (mol%)	–	79	–
O_2 (mol%)	–	21	–
H_2O (mass%)	–	–	96.5
NaCl (mass%)	–	–	3.5
Temperature (°C)	25	25	25
Pressure (bar)	1.013	1.013	1.013

error (the relative difference between the iteration used and the one before) tolerance of 0.01%. For validation, the model was used to simulate the performance of an MED-TVC and of a CRGT, separately, and as shown in Sections 3.2 and 3.3 the simulation results compared very well to available data.

The RK-SOAVE, STEAM-TA and ELECNRTL physical properties (available in ASPEN PLUS) are selected for dealing with the processes where the working media are gas, water and saline water respectively (according to the instruction of ASPEN PLUS), and the main assumptions for cogeneration system simulation are summarized in Table 2.

3.2. CRGT model validation

A turbine blade-cooling model presented in Ref. [7] was incorporated into the simulation model. The MSR is modeled as a Gibbs reactor, which determines the equilibrium conditions by minimizing Gibbs free energy, while the chemical nonequilibrium effects due to reaction kinetics are modeled using the chemical approach temperature difference ΔT_{eq}. [10], which can either be specified or calculated from the following equations for a typical reformer using a nickel-based catalyst [2]:

$$\Delta T_{eq} = 0 \quad \text{if } T_{syn} \geq 923\ \text{K} \tag{2}$$

$$\Delta T_{eq} = 43.33 \times \left[1 - (T_{syn} - 273)/650\right] \text{ if } T_{syn} < 923\ \text{K} \tag{3}$$

where T_{syn} is the temperature of the produced syngas of the reforming reaction. The thermal efficiency is defined as:

$$\eta = W_{net}/Q_{in} \tag{4}$$

where Q_{in} is the energy of the input fuel and W_{net} is the network output of the power cycle.

Kesser et al. have reported the temperature, pressure and mass flow rates of a basic CRGT configuration [2]. To validate the simulation method used in this paper, a basic CRGT cycle was simulated with the same assumptions and the results were compared with those given in Kesser et al., as shown in Table 3. The comparison shows that the results agree quite well, with relative differences of the key cycle parameters within 3%.

The steam-air mass ratio x is defined as the ration between mass flow rate ratio of the steam sent into the MSR (stream 7 in Fig. 1a) and the inlet air of the CRGT (stream 1 in Fig. 1a):

$$x = m_s/m_{air} = m_7/m_1 \tag{5}$$

It directly affects the methane conversion rate in the MSR and the fuel demand of the CRGT. Ref. [2] shows that it has significant influence on the thermal performance of CRGT cycle; when the inlet air of CRGT is fixed, within a certain range(0∼0.15), a larger x means that more steam is added into the MSR, and the endothermic reaction of steam and methane is strengthened, so more heat energy of flue gas is recovered, resulting in higher thermal efficiency while more water consumption (η increases about 0.8 %-points per 0.01 x added).

3.3. MED-TVC model validation

The mass flow fed to each effect depends on the energy balance and the minimum temperature difference allowed on each effect, 2.5–2.8 °C. The energy and exergy balances are derived with the following assumptions:

(1) equal temperature difference across each effect;
(2) equal boiling point elevation for all effects;

The mixture of the vapor flashed from both accumulated distillate and the brine preheats the seawater fed into each effect. This gives a decrease in temperature across the preheaters, which equal to the temperature drop between the effects [16]. The performance of the TVC is taken from Ref. [17]. In the modeling and simulation, the distillate produced in each effect is considered to be salt free (actual salt concentrations are about 10 ppm, negligible for the purposes of the conducted simulation analyses).

Table 2
Main assumptions for the simulation.

Configurations	Parameters	Value	Source
MSR	Pressure drop (% of inlet pressure)	10	Kesser K.F. et al., 1994[2]
	Minimal heat transfer temperature difference gas/gas ($\Delta T_{p,MSR}$)	20 °C	Kesser K.F. et al., 1994[2]
Turbine	Turbine inlet temperature (*TIT*)	1308 °C	Kesser K.F. et al., 1994[2]
	Isentropic efficiency ($\eta_{isn,T}$)	88%	Kesser K.F. et al., 1994[2]
HRSG	Pressure drop (% of inlet pressure)	3	Kesser K.F. et al., 1994[2]
	Minimum heat transfer temperature difference ($\Delta T_{p,HRSG}$)	20 °C (15 °C) gas/gas(liquid)	
	Minimal outlet flue gas temperature (t_f)	90 °C	Kesser K.F. et al., 1994[2]
Compressors	Isentropic efficiency ($\eta_{isn,C}$)	89%	Kesser K.F. et al., 1994[2]
	Compression ratio (π)	15	Kesser K.F. et al., 1994[2]
Combustor	Pressure loss (% of inlet pressure)	3	Kesser K.F. et al., 1994[2]
Pump	Efficiency (η_P)	85%	
MED-TVC	Number of effects (n)	9	
	Temperature drop/effect (ΔT)	3.8 °C	Alasfour F.N. et al., 2005[16]
	Boiling point elevation (*BPE*)	0.8 °C	Alasfour F.N. et al., 2005[16]
	Top brine temperature (*TBT*)	65.6 °C	Alasfour F.N. et al., 2005[16]
	Motive steam temperature (t_m)	140 °C (Saturated, 3.61 bar)	Darwish M. A. et al., 2003[15]
	Entrained steam temperature (t_{en})	49.0 °C (Saturated)	Alasfour F.N. et al., 2005[16]
	Heating steam temperature (t_h)	69 °C (Saturated)	Alasfour F.N. et al., 2005[16]
Ambient state	Temperature (t_a)	25 °C	
	Pressure(P_a)	1.013 bar	

Table 3
Data summary for our simulation CRGT validation (The state point numbers refer to Fig. 1a).

CRGT Parameters		Ref. [2]	ASPEN PLUS
Air compressor inlet air state (State point 1)	m_1/m_{air} [a]	1	1
	t_1 [a]	15 °C	15 °C
	P_1 [a]	0.987 atm	0.987 atm
CH_4 compressor inlet CH_4 state (State point 3)	m_3/m_{air} [a]	0.021	0.021
	t_3 [a]	15 °C	15 °C
	P_3 [a]	4.93 atm	4.93 atm
HRSG inlet water state (State point 5)	m_5/m_{air} [a]	0.144	0.144
	t_5 [a]	15 °C	15 °C
	P_5 [a]	1.97 atm	1.97 atm
MSR (State point 9)	Outlet syngas temperature (T_{syn}) [a]	576 °C	569 °C
HRSG outlet flue gas state (State point 13)	m_{13}/m_{air}	1.155	1.155
	t_{13}	140 °C	140 °C
	P_{13}	1.00 atm	1.00 atm
HRSG	Minimal heat transfer temperature difference ($\Delta T_{p,HRSG}$)	15.7 °C	14.4 °C
Turbine outlet exhaust gas state (State point 11)	m_{11}/m_{air}	1.155	1.155
	t_{11}	596 °C	589 °C
	P_{11}	1.04 atm	1.04 atm
Overall cycle parameters	Steam-Methane mole ratio (R_{SN}) [a]	6.1	6.1
	Specific work output (w)	516 kJ/kg	503 kJ/kg
	Thermal efficiency (η)	48.8%	47.8%

[a] Input variables.

To characterize the performance of the MED-TVC, the performance ratio PR has been defined as Eq. (1). The specific heat transfer area, a, is defined as the heat transfer area needed to produce 1 kg/s fresh water:

$$a = A/m_w \tag{6}$$

where A is the total heat transfer area of the desalination unit, composed of the area of the effects A_E, the condensation area of the end condenser A_C and the area of the preheaters A_{PHE}. To calculate their values, the heat transfer coefficients U of the evaporators, condensers, and preheaters are taken from Ref. [26] (see Appendix A), the temperature approaches ΔT (taken as the logarithmic temperature differences) have been designed, and the heat duty Q is gotten from the simulation case with ASPEN PLUS. The areas can be figured out by:

$$A = Q/(U \cdot \Delta T) \tag{7}$$

The specific exergy consumption, e_{con}, is defined as the exergy consumed for producing 1 kg fresh water:

$$e_{con} = m_m(e_m - e_{cm})/m_w = m_m(e_{16} - e_{14})/m_w \tag{8}$$

where e_m is the specific exergy of the motive steam, and e_{cm} is that of the condensate of the motive steam. Similarly, the specific energy consumption, q_{con}, is defined as the energy consumed for producing 1 kg fresh water:

$$q_{con} = m_m(h_m - h_{cm})/m_w = m_m(h_{16} - h_{14})/m_w \tag{9}$$

where h_m is the specific enthalpy of the motive steam, and h_{cm} is that of the condensate of the motive steam.

Using the model developed by the authors, PR, a_E and e_{con} are calculated under the same conditions as those previously given in Ref. [16], in which the simulated configurations have the same operating conditions of an existing plant in the United Arab Emirates (the Umm A1-Nar plant). The results are shown in Table 4. It can be seen that the relative differences are no more than 3.6%, proving that the model predictions compared well with the data in the reference literature.

Table 4
Data summary for the ASPEN PLUS MED-TVC check case.

MED-TVC Parameters	Ref. [16]	ASPEN PLUS
Number of effects (n) [a]	6	6
Top brine temperature (TBT) [a]	61.8 °C	61.8 °C
Temperature drop/effect (ΔT) [a]	3.8 °C	3.8 °C
Boiling point elevation (BPE) [a]	0.8 °C	0.8 °C
Motive steam pressure (P_m) [a]	25 bar	25 bar
Heating steam temperature (t_h) [a]	65 °C	65 °C
Feed seawater temperature (t_{feed}) [a]	40 °C	40 °C
Cooling seawater temperature (t_{sea}) [a]	30 °C	30 °C
Motive steam/Entrained steam (mass flow)	1.36	1.36
Performanceratio (PR)	10.05	10.04
Specific heat transfer area of the effects (a_E)	326.2 m^2/(kg/s)	338.1 m^2/(kg/s)
Specific exergy consumption(e_{con})	87.91 kJ/kg	88.23 kJ/kg
Specific energy consumption(q_{con})	252.87 kJ/kg	253.02 kJ/kg

[a] Input variables.

4. The cogeneration system performance and discussion

4.1. Evaluation criteria

The system has two useful products: power and fresh water. To characterize the cogeneration performance, the power-to-water ratio R_{pw} is introduced. It is defined as the net generated power W_{net} divided by the mass flow rate of the produced water m_w:

$$W_{net} = W_T - W_{COM} - W_P \tag{10}$$

$$R_{pw} = W_{net}/m_w \tag{11}$$

where W_T is the work output of the turbine, and the W_{COM} and W_P is work consumed by compressors and pumps, respectively.

The exergy efficiency of the dual-purpose system ε is calculated as the exergy output divided by the exergy input:

$$\varepsilon = (W_{net} + E_w)/E_{in} \tag{12}$$

where E_{in} represents the exergy of the input NG, and E_w is the exergy of the water production, which is given as the minimal work needed in a reversible separation process for producing the same amount of fresh water as in the cogeneration system [13].

The ratio of water used for the reformer (m_s, stream 7 in Fig. 1a) to the total water produced by the MED ($m_{w,tol}$, stream 17 in Fig. 1a) is defined as CRGT-consumed water ratio δ:

$$\delta = m_s/m_{w,tol} = m_7/m_{17} \tag{13}$$

4.2. Cogeneration system performance

Mainstream states of the cogeneration system including temperature, pressure, mass flow rate, vapor fraction and chemical composition are presented in Table 5.

The performance results are reported in Table 6. The thermal efficiency η of top cycle CRGT is 47.0%, and the performance ratio PR of the button cycle MED-TVC is 11.3. For the integrated system, the power-to-water ratio R_{pw} is 745 kJ/kg and the exergy efficiency ε is 45.7%. Table 7 shows the exergy destruction of different components in the cogeneration system in detail. The component exergy change is defined as the change in exergy between the entry state and the exhaust state of each process.

If the HRSG did not generate the motive steam, its exergy destruction would decline from 61.9 MW to 58.4 MW; however, the exergy loss of the flue gas would increase from 50.0 MW to 102.9 MW. The integration of the MED-TVC into the CRGT cycle is of great benefit to decrease the exergy loss of the flue gas and recover the exhaust heat to produce large amounts of fresh water.

Table 5
Mainstream states of the CRGT+MED dual-purpose system.

No.	t (°C)	p (bar)	m (kg/s)	Vapor fraction	Molar composition							
					N_2	O_2	CH_4	CO	H_2	CO_2	H_2O	NaCl
1	25	1.01	1000	1	0.79	0.21						
2	399	14.9	777	1	0.79	0.21						
3	25	1.01	20.7	1			1					
4	140	21.3	20.7	1			1					
5	25	3.0	120	0							1	
6	25.1	22.5	120	0							1	
7	474	21.4	120	1							1	
8	407	21.3	141	1			0.162				0.838	
9	567	19.2	141	1			0.101	0.004	0.183	0.043	0.669	
10	1308	14.6	918	1	0.610	0.088				0.037	0.265	
11	587	1.05	1131	1	0.641	0.109				0.031	0.219	
12	494	1.03	1131	1	0.641	0.109				0.031	0.219	
13	96.8	1.01	1131	1	0.641	0.109				0.031	0.219	
14	65.6	0.3	58.4	0							1	
15	65.6	3.75	58.4	0							1	
16	140	3.61	58.4	1							1	
17	25	3.0	660	0							1	
18	25	3.0	540	0							1	
20	35.1	3.0	144	0							0.934	0.066
22	69	0.3	89.6	1							1	
23	49	0.12	31.2	1							1	
24	32.4	3.0	804	0							0.989	0.011

Fig. 2 is the t-Q diagram of the exhaust heat recovery process. The turbine exhaust heat is recovered in a high-to-low temperature cascade. The horizontal-line segments (a) and (b) represent the isothermal evaporation processes of the water streams (6) and (15), respectively. The stream (6) is the water supply for CRGT cycle and the stream (15) is heated to be the motive steam to drive MED-TVC. It can be seen that owing to the integration of MED-TVC into the CRGT, the heat recovery in HRSG is enhanced by stream (15) and the thermal match between the heating and heated streams gets better. However, the temperature difference along (a) and to the left is still large and leading to exergy losses, which needs further improvement.

The exergy analyze in Table 7 also provides some guidance for system performance improvement. The combustion-associated exergy change is as usual the biggest item. This destruction can be straightforwardly decreased by enhancing the reforming reaction (elevating the fuel heating value) or increasing the inlet temperature of gas turbine beyond the assumed 1308 °C. For example, the former can be realized by increasing the steam led into the MSR. When the mass flow of air is fixed, the increase of steam-air ratio x will result in the elevation of output network (see Section 6.1). The latter would be possible if a more advanced turbine is used. The turbine expansion progress causes the next largest exergy destruction, which can be reduced by using a more efficient turbine as well. The exergy destruction of HRSG is a bit less than that of gas turbine. This destruction can be weakened by decreasing the temperature differences between the heat exchanging streams, but this would obviously require larger or/and more complex heat exchangers [10].

Table 6
CRGT+MED dual-purpose system performance summary.

CRGT section	Compressor inlet air mass flow rate[a]	1000 kg/s
	Steam-air mass ratio (x) [a]	0.12
	Steam-NG mole ratio (R_{SN})	5.16
	NG conversion rate (R_{NC})	31.7%
	Work output (w)	494.1 MW
	Thermal efficiency of the top cycle (η)	47.0%
MED-TVC section	Performance ratio (PR)	11.3
	Specific heat transfer area (a)	337 m^2/(kg/s)
	Specific exergy consumption (e_{con})	54.0 kJ/kg
	Specific energy consumption (q_{con})	216 kJ/kg
	Water production ($m_{w,tol}$)	660 kg/s
	Water sent to CRGT (m_s)	120 kg/s
Cogeneration system	Fuel energy input (Q_{in})	1051 MW
	Fuel exergy input (E_{in})	1078 MW
	Work consumption for MED-TVC	2.61 MW
	Net work output (W_{net})	491.5 MW
	Net water production (m_w)	540 kg/s
	CRGT-consumed water ratio (δ)	18.2%
	Water exergy (E_w)	1.50 MW
	Power-to-water ratio (R_{pw})	745 kJ/kg
	Exergy efficiency (ε)	45.7%

[a] Input variables.

5. Comparison with other cogeneration systems

To determine whether the proposed dual-purpose system, CRGT integrated with MED-TVC (CRGT + MED), has an advantage over the existing commonly used dual-purpose systems, we have performed a performance comparison with four cogeneration systems, including the older, widely used Rankine power generation system having a backpressure ST) with an MSF desalination plant (ST + MSF) [27–31], the ST plus MED (ST + MED), the more modern

Table 7
Exergy analysis of the CRGT+MED dual-purpose system.

Configuration	Amount(MW)	Percentage
Exergy input		
Natural gas	1078.0	100.00%
Exergy output		
Net power output	491.5	45.59%
Fresh water	1.5	0.14%
Exergy destruction		
Combustor	317.9	29.49%
Methane steam reformer (MSR)	10.0	0.93%
Compressors and pumps	28.8	2.68%
Gas turbine	63.9	5.93%
HRSG	61.9	5.74%
Mixer	11.1	1.03%
Thermal vapor compressor (TVC)	15.4	1.43%
Multi-effect desalination (MED)	21.1	1.96%
Flue gas	50.0	4.63%
Brine	0.7	0.07%
Mechanical and generator losses	4.3	0.39%
Exergy efficiency	–	45.7%

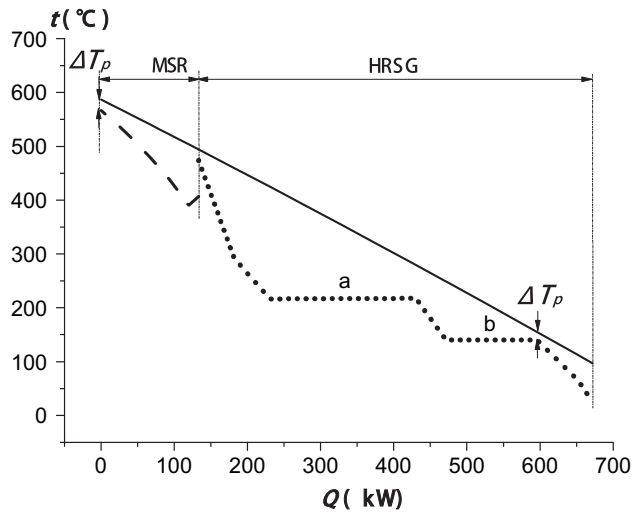

Fig. 2. The heat recuperation *t*-*Q* diagram of the CRGT+MED dual-purpose system.

highest efficiency dual-purpose system comprised of a CC with backpressure steam turbine and an MSF desalination plant (CC + MSF) [15], and the CC plus MED (CC + MED) [12]. In the comparison analysis all systems are assumed to consume methane at the same flow rate for a comparison base.

The reference MSF system considered here has the characteristics given in Table 8 [29]. It is operated at a maximum brine temperature of 90 °C, a heating steam temperature of 100 °C and a *PR* of 8. For the water production as large as possible, all steam of the ST/CC topping cycle is extracted to drive the MED/MSF bottom cycle.

5.1. Comparison with ST + MED and ST + MSF

In the ST plant, the parameters of the main steam are set to be 535 °C, 161.8 bar. The thermal efficiency of the boiler is 98%, and the thermal efficiency of the whole system is 37% (the common parameters of subcritical power units in China).

When the methane flow rate is 20.7 kg/s (as the same as that in CRGT), the main-steam flow rate is calculated to be 315 kg/s by energy balance. As the heating steam of the MSF directly comes from the steam turbine after the expansion process, the backpressure rises from original 0.085 bar–1.012 bar (100 °C), which is chosen for being equal to the heating steam temperature in Table 8. By simulating the turbine model with an isentropic efficiency of 80% in ASPEN PLUS, the work output drops from 388.7 MW to 309.9 MW. As a result, the thermal efficiency of the Rankine steam power cycle decreases from 37% to 29.5% (Table 9), and the mass flow rate of the heating steam in MSF is 315 kg/s.

Similarly, when the backpressure ST is integrated with MED, the backpressure rises from original 0.085 bar–3.61 bar (140 °C), which are the parameters of the motive steam in MED (Table 2). After simulation with ASPEN PLUS, the turbine power output reduces from 388.7 MW to 260.5 MW. Eventually, the thermal efficiency of the Rankine steam power cycle decreases from 37% to 24.8% (Table 9), and the motive steam of MED is also 315 kg/s.

The comparison results of the CRGT + MED, ST + MED and ST + MSF systems are exhibited in Table 9.

Compared to the ST + MSF system, the CRGT + MED system has 76% higher power output and 79% less water production with the same energy input. The reason is that the CRGT is much more efficient than the Rankine steam power cycle; although the performance ratio *PR* of MED is larger than that of MSF, the flow rate of the motive steam sent into MED (140 °C steam, 58.4 kg/s) is smaller than that fed into MSF (100 °C steam, 315 kg/s), limited by exhaust heat recuperation in CRGT, leading the smaller m_w of the MED. As the exergy of the power is much larger than that of the water production, the exergy efficiency mainly depends on the power output. Hence the exergy efficiency of the CRGT + MED cogeneration system is higher than that of the ST + MSF one.

The power output of the ST + MED system is the lowest in the three cogeneration systems, and hereby its exergy efficiency is the worst. However, its fresh water production is the highest, for it has the *PR* of 11.3 (larger than 8 of MSF), the motive steam mass flow rate of 315 kg/s (larger than 58.4 kg/s of CRGT- cogeneration systems), and no water supply for the top cycle (like the CRGT).

It is noteworthy that comparing the CRGT + MED dual-purpose system with the ST- cogeneration systems, the MED bottom cycle did not decrease the efficiency of the CRGT top cycle; it just recovered the surplus exhaust gas heat after the reforming steam recuperated its needed flue gas waste heat. Although the water production of CRGT + MED is the least, its electricity output is the most and the exergy efficiency is the highest. What is more, the MED subsystem in CRGT + MED has the least total energy consumption and heat transfer area among the dual-purpose units.

In addition, in the industry the MED system generally requires less heat transfer area than MSF, but in this research the MED has a larger specific heat transfer area than that of MSF. The explanation is as following. Assume the water production of the two systems is just the same, 1 kg/s. As the specific energy consumption of MED is lower (54.0 kJ/kg VS 57.7 kJ/kg in Table 9), the total energy consumption *Q* of MED is smaller. Since the MED contains the phase-change heat transfer, the heat transfer coefficients *U* of MED are usually larger than those of MSF. However, in MSF the temperature difference between the heating steam and brine (*TBT*) is 10 °C (100°C–90 °C, assumptions in Table 8), while 3.4 °C (69°C–65.6 °C, assumptions in Table 2) in MED, which causes the heat transfer temperature differences ΔT of MED is quite smaller; and hence through Eq. (7) the specific heat transfer area *A* of MED becomes larger.

5.2. Comparison with CC + MED and CC + MSF

With reference to the CC specifications of the S109FA model (GE company, 50 Hz, including a MS9001FA gas turbine and a triple-pressure-reheat steam cycle) [32–35], the CC in this paper was simulated with ASPEN PLUS software. The main assumptions of the gas turbine part are shown in Table 2 (*TIT* = 1308 °C and $\pi = 15$). In the steam cycle, three reheat pressure levels of the HRSG are 140/30/4 bar, the condensation pressure is 0.05 bar, and the steam temperature at turbine admission is 562 °C. Finally, the gas turbine has an exhaust temperature of 587 °C and efficiency of 35.2%; the turbine outlet steam flow rate is 164 kg/s; the CC has a thermal efficiency of 56%, and the system net power output is 588.4 MW.

To provide the 100 °C heating steam for MSF (see Table 8), the backpressure of the steam turbine in the bottom cycle is raised from 0.05 bar to 1.012 bar/100 °C. Therefore, the work output of the above-described CC drops from 588.4 MW to 525.3 MW, and the thermal efficiency decreases to 50.0% (Table 10).

Table 8
Data of the reference MSF plant.

MSF Parameters	Ref. [19]
Top brine temperature (*TBT*)	90 °C
Heating steam temperature (t_h)	100 °C
Distillate output	313.25 kg/s
Number of stages (recovery + rejection)	21 + 3
Performanceratio (*PR*)	8
Specific heat transfer area of the effects (a_E)	292 m^2/(kg/s of water)
Specific exergy consumption(e_{con})	60.84 kJ/kg
Mechanical pumping energy (e_P)	3824 kW

Table 9
Comparison among the CRGT + MED, ST + MED and ST + MSF systems.

System performance		CRGT + MED	ST + MED	ST + MSF
Power section	Fuel energy input (Q_{in})	1051 MW	1051 MW	1051 MW
	Fuel exergy input (E_{in})	1078 MW	1078 MW	1078 MW
	Work output	494.1 MW	260.5 MW	309.9 MW
	Thermal efficiency of the top cycle (η)	47.0%	24.8%	29.5%
Desalination section	Performance ratio (PR)	11.3	11.3	8
	Gross water production	660 kg/s	3560 kg/s	2520 kg/s
	Specific heat transfer area (a)	337 m^2/(kg/s)	337 m^2/(kg/s)	292 m^2/(kg/s)
	Total heat transfer area (A)	222,000 m^2	1199550 m^2	735840 m^2
	Specific energy consumption (q_{con})	216 kJ/kg	216 kJ/kg	301 kJ/kg
	Total energy consumption (Q_{con})	143 MW	768.9 MW	758.5 MW
	Specific exergy consumption (e_{con})	54.0 kJ/kg	54.0 kJ/kg	57.7 kJ/kg
	Total exergy consumption (E_{con})	33.9 MW	192.2 MW	145.4 MW
Cogeneration system	Work consumption for desalination	2.61 MW	14.1 MW	30.8 MW
	Net work output (W_{net})	491.5 MW	246.5 MW	279.2 MW
	Net water production (m_w)	540 kg/s	3560 kg/s	2520 kg/s
	Top-cycle-consumed water ratio (δ)	18.2%	0	0
	Water exergy (W_e)	1.5 MW	9.9 MW	7.0 MW
	Power-to-water ratio (R_{pw})	745 kJ/kg	69.2 kJ/kg	111 kJ/kg
	Exergy efficiency (ε)	45.7%	23.8%	26.5%

Similarly, when the backpressure CC is integrated with MED, the backpressure of the steam turbine rises from the original 0.05 bar–3.61 bar (140 °C), the motive steam parameters of MED (Table 2). In the simulation, the CC power output drops from 588.4 MW to 481.1 MW. Hence the thermal efficiency of the CC decreases from 56% to 45.8% (Table 10), and the motive steam of MED is 164 kg/s.

The comparison results of the CRGT + MED, CC + MED and CC + MSF systems are summarized in Table 10.

Both the power output and water production of CC + MSF are larger than those of CRGT + MED. Not only the thermal efficiency of CC is higher than that of CRGT, but also the motive steam mass flow rate of CC + MSF (164 kg/s) is much bigger than that of CRGT + MED (58.4 kg/s). As a result, the thermal performance of the CC + MSF system is better than that of CRGT + MED.

For CC + MED system, the elevation of the steam turbine backpressure makes the thermal efficiency of the CC subcycle decline by 10.2%-points, so the work output of CC + MED become less than that of CRGT + MED and the exergy efficiency is also lower. In the three cogeneration systems, the power output of CC + MED is the lowest, but its water production is the highest. The reason is as the same as that of the ST + MED system compared to the CRGT + MED and ST + MSF systems in Section 5.1.

From Sections 5.1 and 5.2, it can be seen that with the same energy input, the power and water productions of the five cogeneration systems are quite different from each other. The CRGT + MED system has the second highest work output, the lowest water production, and the least total heat transfer area. As the exergy of the fresh water is too small, the exergy efficiency ε mainly emphasizes the power output of the dual-purpose system; so the ε is not enough to describe the advantages and disadvantages of the cogeneration systems. For example, the ST + MED system has the lowest ε, but its water production is the largest. To compare the performances of the cogeneration systems completely, the further economic study was carried on.

5.3. Economic perspective

The economic analysis was based on the following assumptions:

- The price of NG is 4.24\$/MMBtu (0.14\$/Nm^3) for power generation [36], assumed to be constant over the life of the system.
- The annual running time H is 7000 h per year, and the plant life n is 20 years [30].
- The discount rate i is 8% [31].
- No loan is made for the total plant investment.

Table 10
Comparison among the CRGT + MED, CC + MED and CC + MSF systems.

System performance		CRGT + MED	CC + MED	CC + MSF
Power section	Fuel energy input (Q_{in})	1051 MW	1051 MW	1051 MW
	Fuel exergy input (E_{in})	1078 MW	1078 MW	1078 MW
	Work output	494.1 MW	481.1 MW	525.3 MW
	Thermal efficiency of the top cycle (η)	47.0%	45.8%	50.0%
Desalination section	Performance ratio (PR)	11.3	11.3	8
	Gross water production	660 kg/s	1850 kg/s	1310 kg/s
	Specific heat transfer area (a)	337 m^2/(kg/s)	337 m^2/kg	292 m^2/(kg/s)
	Total heat transfer area (A)	222,000 m^2	623450 m^2	382520 m^2
	Specific energy consumption (q_{con})	216 kJ/kg	216 kJ/kg	301 kJ/kg
	Total energy consumption (Q_{con})	143 MW	400 MW	394 MW
	Specific exergy consumption (e_{con})	54.0 kJ/kg	54.0 kJ/kg	57.7 kJ/kg
	Total exergy consumption (E_{con})	33.9 MW	100 MW	75.6 MW
Cogeneration system	Work consumption for desalination	2.61 MW	7.33 MW	16.0 MW
	Net work output (W_{net})	491.5 MW	473.7 MW	509.3 MW
	Net water production (m_w)	540 kg/s	1850 kg/s	1310 kg/s
	Top-cycle-consumed water ratio (δ)	18.2%	0	0
	Water exergy (E_w)	1.5 MW	5.1 MW	3.6 MW
	Power-to-water ratio (R_{pw})	745 kJ/kg	256 kJ/kg	389 kJ/kg
	Exergy efficiency (ε)	45.7%	44.4%	47.6%

- The price of electricity is 0.08$/kWh [37].
- The price of water is 0.7$/m^3 [38].

BOP (Balance of plant) consists of the remaining systems, components, and structures that comprise a complete power plant or energy system that is not included in the prime mover. For a conventional power generation system, the *BOP* is usually assumed to be 15% of the known components' cost [39]. The term O&M is the cost of operating and maintenance, assumed to be 4% of the first cost of the system [40]. However, due to the upkeep and maintenance of the reformer (including the catalyst), the *BOP* of the CRGT is assumed to be 20% of the main components' cost and the O&M cost increases to be 10% of the first cost [33,40,41]. Taxes and insurance are not considered in this evaluation.

The investment estimation of the five dual-purpose systems is listed in Table 11. With the same mass flow of CH_4 input, we can find that the capital cost of CRGT + MED system is the lowest; however, the quite different capacities of the systems (especially the seawater desalination subsystems) have significant influence on the total plant cost. For instance, the MED-TVC in CRGT + MED only costs 86676k$ (the least in the desalination subsystems), but its water product is also the lowest, just 660 kg/s. To compare the economic performances of the cogeneration systems, the *COE* (electricity cost), *COW* (fresh water cost), and *PBP* (payback period) of the systems should be analyzed.

Table 11
Investment cost of the dual-purpose systems.

Plant configuration	Price	Capacity	Investment cost[$10^3$$]
CRGT + MED			
Simple cycle section[a]	212$/kW[32]	494.1 MW	104,758
MSR[b]	29$/kW[33,40,41]	133.2 MW	3864
HRSG[c]	244$/m^2[39,40,42]	81,406 m^2	19,863
CRGT section	–	–	128485
MED-TVC	1520$/(m^3/day)[15,24]	660 kg/s	86,676
Total plant cost	–	–	215,161
ST + MED			
Boiler[d]	20$/kW	1031 MW	20,322
Steam turbine and generator[e]	–	388.7 MW	17,608
Balance of plant[f]	–	–	5689
ST section	–	–	43,619
MED-TVC	1520$/(m^3/day) [15,24]	3560 kg/s	467,462
Total plant cost	–	–	511,081
ST + MSF			
Boiler	20$/kW	1031 MW	20,322
Steam turbine and generator	–	388.7 MW	17,608
BOP	–	–	5689
ST section	–	–	43,619
MSF	1615$/(m^3/day)[30,31]	2520 kg/s	351,631
Total plant cost	–	–	395,250
CC + MED			
CC section[g]	501$/kW[32]	588.4 MW	294,765
MED-TVC	1520$/(m^3/day) [15,24]	1850 kg/s	242,957
Total plant cost	–	–	537,722
CC + MSF			
CC section	501$/kW[32]	588.4 MW	294,765
MSF	1615$/(m^3/day) [30,31]	1310 kg/s	182,792
Total plant cost	–	–	477,557

[a] Combustor, gas turbine, generator, compressors, and *BOP* are included. The unit cost is taken from the simple cycle specifications of the PG9351FA model (GE company, 50 Hz) [32].

[b] Ni-based catalyst is set inside. As the reforming reaction is in the moderate-temperature range (407–567 °C), the unit cost of MSR is quite lower than that of the high temperature reforming reactor in traditional hydrogen-producing process [33,40,41].

[c] The heat transfer area is calculated by Eq. (7). The heat duty Q and temperature approaches ΔT (taken as the mean temperature difference) are gotten from the simulation case with ASPEN PLUS. The heat transfer coefficients U, 99 W/(m^2 °C), and unit cost are taken from the research in Ref. [42].

[d] Shanghai Boiler Factory was consulted for the unit cost of the boilers. The exchange rate of conversion from RMB to US dollars is 7.

[e] Hangzhou Steam Turbine Factory was consulted for the investment cost, according to the capacity of the steam turbine in the ST + MED/MSF cases. The RMB/USD foreign exchange rate is 7.

[f] As the ST system is just a conventional power generation system, we assumed the *BOP* accounts for 15% of the known component cost of the system [37,43].

[g] Combustor, gas turbine, HRSG, steam turbine, generator, compressors, and *BOP* are included. The unit cost is taken from the CC specifications of the S109FA model (GE company, 50 Hz, including a MS9001FA gas turbine and a triple-pressure-reheat steam cycle) [32].

The *COE* of the dual-purpose systems is calculated as:

$$COE = \left(\beta \cdot TPC_{\text{pow}} + C_{\text{om,pow}} + C_{\text{fu,pow}}\right) \Big/ \left(H \cdot W_{\text{net,pow}}\right) \quad (14)$$

The numerator is the annual average electricity cost. TPC_{pow} is the total plant cost of the power subsystems (CRGT, ST and CC). β is the annual average investment coefficient, a function of the discount rate i and plant life n:

$$\beta = i \Big/ \left[1 - (1 + i)^{-n}\right] \quad (15)$$

$C_{\text{om,pow}}$ is the annual O&M cost of the power subsystems. It should be noted that $C_{\text{fu,pow}}$ is the annual fuel cost of the cogeneration systems, while $W_{\text{net,pow}}$ is the hypothetical power output of the power subsystems without steam extraction or pump-work supply for desalination plants ($W_{\text{net,pow}}$ of CRGT, ST and CC are 494.1 MW, 388.7 MW and 588.4 MW respectively, see Section 4.1, 5.1 and 5.2). In other words *COE* distributed in this way is just the electricity cost of the power separate generation systems with the same configuration as the power subsystems in the cogeneration systems.

By deducting the electricity cost from the whole product cost, the cost of the fresh water *COW* is calculated as:

$$COW = \left(\beta \cdot TPC + C_{\text{om}} + C_{\text{fu}} - H \cdot W_{\text{net}} \cdot COE\right) \Big/ \left(H \cdot m_{\text{W}}\right) \quad (16)$$

TPC, C_{om} and C_{fu} are the total cost, annual O&M cost and fuel cost of the cogeneration systems respectively. W_{net} and m_{W} are the net product outputs of the cogeneration systems.

The payback period *PBP* is the time by which all the revenue of the plant will have become equal to the investment *TPC* [42,43]:

$$R \cdot \left[(1+i)^{PBP} - 1\right] \Big/ \left[i(1+i)^{PBP}\right] = TPC \quad (17)$$

R is the annual net revenue of the plant:

$$R = R_{\text{e}} + R_{\text{w}} - C_{\text{fu}} - C_{\text{om}} \quad (18)$$

R_{e} and R_W are the annual revenue of the net power and water product, defined as the output multiplied by the corresponding price.

Table 12 presents the comparison results. It is shown that the *COE* () of the CRGT- cogeneration system is higher than that of CC- ones (0.0419$/kWh vs. 0.0400$/kWh), while both are lower than that of ST- systems (0.0426$/kWh). Because the efficiency of CC (56%) is higher than that of CRGT (47%), although the former configuration is far more complicated, which costs much more capital investment, its *COE* achieves the lowest yet. For all the power subsystems, the annual fuel cost $C_{fu,pow}$ occupies the most of the annual average electricity cost (64%~90%), and followed by the annual average investment $\beta \cdot TPC_{pow}$ (4%~18%) and annual O&M cost $C_{om,pow}$ (6%~18%).

The *COW* of the CRGT + MED is the lowest in the five dual-purpose systems (1.28$/t). That is because the generation of the motive steam just uses the surplus exhaust gas heat, so as not to reduce the power output of the CRGT power cycle; the deducted electricity cost from the total product cost is quite large and the water cost part is relatively small. On the contrary, due to the steam

Table 12
Comparison of electricity and fresh water cost and payback period.

Items	Investment (10^3\$)	Work output (MW)	*COE* (\$/kWh)	Water output (kg/s)	*COW* (\$/t)	*R* (10^3\$)	*PBP* (y)
CRGT + MED	215,161	491.5	0.0419	540	1.28	81,577	3.9
ST + MED	511,081	246.5	0.0426	3560	1.50	61,896	14.0
ST + MSF	395,250	279.2	0.0426	2520	1.60	75,753	7.0
CC + MED	537,722	473.7	0.0400	1850	1.74	105,937	6.8
CC + MSF	477,557	509.3	0.0400	1310	1.79	119,839	4.9

extraction for running MED/MSF, the network output of ST/CC power subsystems decreases greatly; the water cost has a high proportion of the total cost. Besides, the less *TPC* of CRGT-MED system is also in favor of the lower *COW*.

Compared with the CC- cogeneration systems, the fresh water of the ST- ones cost a little less; the main reasons are the total plant cost is relatively low and the water output is pretty large.

The low *TPC* and high revenue of CRGT + MED system result in its shortest *PBP* in the five cogeneration systems (3.9 years). The revenue of CC + MED/MSF system is remarkable, but its high *TPC* makes the *PBP* (6.8/4.9 years) longer than that of CRGT + MED; however, it is still shorter than that of ST + MED/MSF (14.0/7.0 years).

Compared to the ST + MED/MSF and CC + MED/MSF cogeneration systems, the CRGT + MED system has lower product cost and shorter payback period. Hence the CRGT + MED dual-purpose system is considered to be feasible and attractive for power and water cogeneration.

6. Parametric sensitivity analysis of the cogeneration system

As the steam-air mass ratio x has a strong effect on the thermal performance of a CRGT, and both the temperature of the motive steam t_m and the number of effects n directly affect the *PR* of the MED-TVC, a parametric analysis was carried out to investigate their influence on the performance of the cogeneration system.

In the Fig. 3(a), 4(a) and 5(a), the input fuel energy Q_{in}, net work output W_{net} and mass flow rate of the produced water m_w are normalized by the corresponding values of the base cycle (see

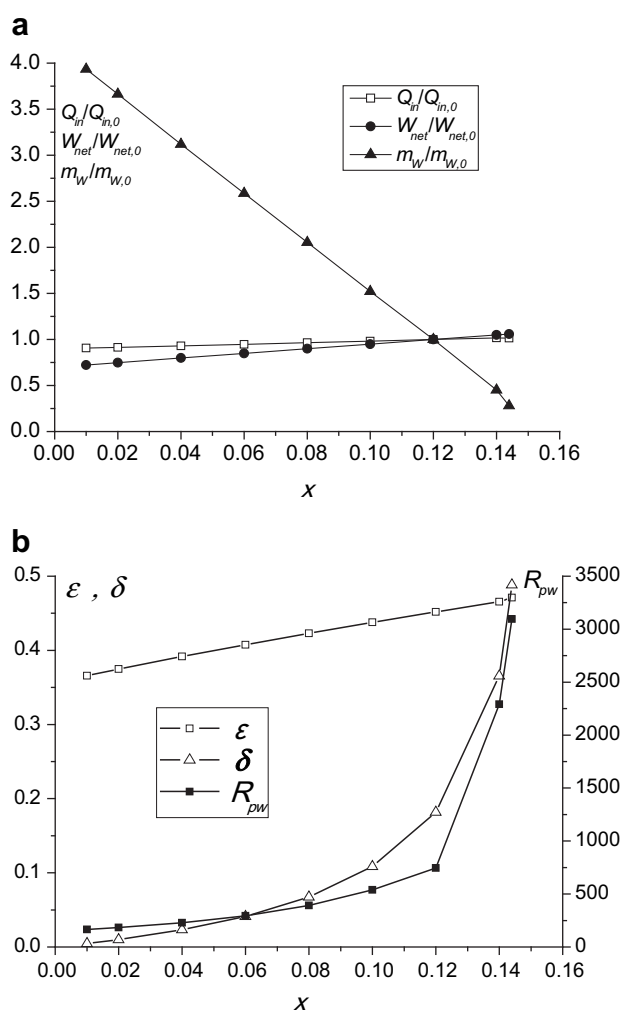

Fig. 3. a. The effect of the steam-air ratio x on normalized energy input $Q_{in}/Q_{in,0}$, power output $W_{net}/W_{net,0}$ and water production $m_w/m_{w,0}$, b. The effect of the steam-air ratio x on exergy efficiency ε, CRGT-consumed water ratio δ and power-to-water ratio R_{pw}.

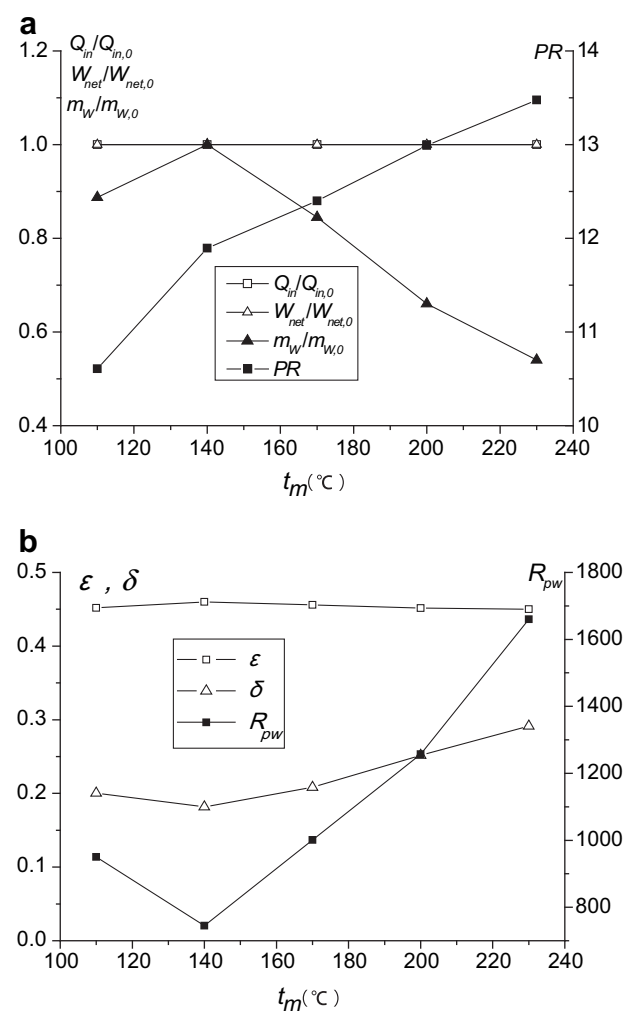

Fig. 4. a. The effect of the temperature of the motive steam t_m on normalized energy input $Q_{in}/Q_{in,0}$, power output $W_{net}/W_{net,0}$, water production $m_w/m_{w,0}$, and performance ratio *PR* b. The effect of the temperature of the motive steam t_m on exergy efficiency ε, CRGT-consumed water ratio δ and power-to-water ratio R_{pw}.

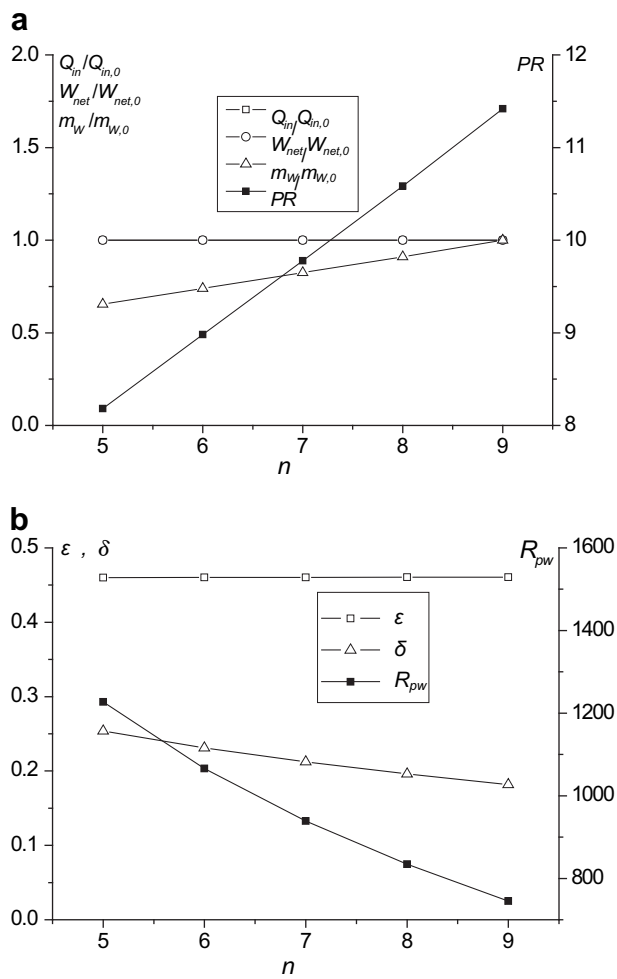

Fig. 5. a. The influence of the number of the MED effects n on normalized energy input $Q_{in}/Q_{in,o}$, power output $W_{net}/W_{net,0}$ water production $W_{net}/W_{net,0}$ and performance ratio PR b. The influence of the number of the MED effects n on exergy efficiency ε, CRGT-consumed water ratio δ and power-to-water ratio R_{pw}.

section 4.2), so that the change trend of them can be exhibited more clearly in one figure.

6.1. Influence of the steam-air ratio x

Fig. 3 shows the influence of x on Q_{in}, W_{net}, m_w, ε, δ and R_{pw} when the inlet air m_{air} is fixed.

An increasing x implies more steam sent into the MSR. Since the *TIT*, the minimum heat transfer temperature differences in MSR, HRSG and MED are kept constant, increasing steam reactant causes an increase of input fuel energy Q_{in}. Due to the increase of the working fluid flowing through the turbine, W_{net} is increased.

As more steam is introduced to MSR, the steam-NG mole ratio (R_{SN}) is enhanced, the endothermic reaction of steam and methane is strengthened, more heat energy of flue gas is recovered and the methane conversion recovers more exhaust heat for reforming, which results in less energy left for the motive steam generation in HRSG. With a fixed MED-TVC configuration and t_m, decreasing production of the motive steam causes the decline of the water production m_w.

The decrease in m_w and increase in W_{net} make the power-to-water ratio R_{pw} go up. Meanwhile, the increasing steam sent into MSR and decreasing water production cause the CRGT-consumed water ratio δ move up rapidly.

Since the exergy of the water only accounts for a small portion of the total production exergy ($W_{net} + E_W$), the exergy efficiency ε mainly depends on W_{net} and Q_{in}. As W_{net} grows faster than Q_{in}, a higher exergy efficiency of the CRGT section is achieved.

It is noted that the maximum steam-air ratio is limited by the constraint on the minimum pinch point temperature difference of 15 °C in HRSG [2]. From Fig. 3a, we can see that when x gets close to 0.15, all the exhaust heat is used for generating steam needed for reforming, none is left for motive steam generation. Hardly any fresh water would thus be produced.

6.2. Influence of the temperature of the motive steam t_m

The motive steam is generated by the surplus exhaust heat after the reforming steam recuperates its needed flue gas waste heat. Since the compressor inlet air mass flow rate, steam-air mass ratio x, *TIT*, minimum heat transfer temperature differences in MSR, HRSG and MED are fixed, the steam sent into the MSR, surplus exhaust heat for motive steam generation, the work output of the CRGT cycle and Q_{in} are kept the same (Fig. 4a). Hence if the motive steam temperature is raised, its flow rate will come down.

An increasing t_m implies less motive steam and a higher performance ratio PR (Fig. 4a). The increase of PR and drop of m_m have opposite effects on the water production. As a result, the m_w increases and reaches a maximum, at $t_m = 140$ °C among the calculated points and decreases afterwards.

Although the change of the pumping work of MED has the same trend as that of m_w, for the pumping work is rather small compared to the work output of the CRGT, W_{net} shows little change in Fig. 4a.

As a result of the changes of the W_{net} and m_m, R_{pw} becomes minimal and the ε maximal when t_m is 140 °C (Fig. 4b).

When t_m is 140 °C, the CRGT-consumed water ratio δ also reaches the minimum due to the trend of m_w and the invariability of steam sent into MSR (Fig. 4b).

6.3. Influence of the number of MED effects n

The number of effects n does not affect the thermal performances of the top CRGT cycle. When n is increased, the motive steam generation in HRSG, the work output of the CRGT and Q_{in} (Fig. 5a) are changeless.

While the n is increasing, the PR moves up, and the m_w rises (Fig. 5a). Although the power consumption of pumps goes up in MED, it is still much less than the work output of the CRGT. So the decrease of W_{net} is quite inconspicuous (Fig. 5a).

Due to the change trends of the W_{net} and m_w, the power-to-water ratio R_{pw} decreases. The CRGT-consumed water ratio δ also declines because the steam sent into MSR keeps the same but the m_w rises. Since the increase of the exergy of the water production is not remarkably and the W_{net} has a little decrease, the increase of the exergy efficiency of the cogeneration system is quite restricted (Fig. 5b), 0.012% per effect added. It can be seen that n mainly affects the performance of the MED part in the cogeneration system. The cost of water *COW* was figured out to decrease 0.02 ~ 0.03$ per effect added, for the water output grows faster than the investment of the MED subsystem while n increasing.

7. Conclusions

This paper proposed and analyzed a novel cogeneration dual-purpose system, which integrates a CRGT with the low temperature (65.6 °C) MED-TVC system. The turbine exhaust heat was recovered for generating motive steam to run the MED-TVC, which in turn provided the reforming process with its needed water. The main conclusions include:

(1) In the base case of the compression ratio being 15, turbine inlet temperature being 1308 °C, motive steam temperature being 140 °C, MED-TVC with 9 effects, entrained vapor from the fifth effect, and the steam-air ratio being 0.12, the specific work output, performance ratio, and CRGT-consumed water ratio are 491.5 kJ/kg, 11.3, and 18.2% respectively.

(2) Comparing the CRGT + MED with the ST + MED, ST + MSF, CC + MED and CC + MSF cogeneration systems with the same mass flow rate of input methane,
- The thermal efficiency of CRGT is higher than that of ST but lower than that of CC. Compared to MSF, MED has a higher *PR*, lower specific energy and exergy consumption, while larger specific heat transfer area, owing to its smaller heat-transfer temperature differences.
- The CRGT + MED system has the second highest work output, the lowest water production, and hence the least total heat transfer area.
- The *COE* of the CRGT- cogeneration system is higher than that of CC- ones quite close (0.0419$/kWh vs. 0.0400$/kWh), while both are lower than that of ST- systems (0.0426$/kWh); the *COW* of the CRGT + MED is the lowest, 1.28$/t, while the *COW* of the other dual-purpose systems is in the range 1.50∼1.79$/t; the *PBP* of the CRGT + MED is the shortest.
- From the lower product cost and shorter payback period of CRGT + MED, we can draw the conclusion that the CRGT + MED dual-purpose system is a feasible and attractive choice for power and water cogeneration.

(3) A parametric sensitivity analysis was also conducted to investigate the effects of steam-air mass ratio x, motive steam temperature t_m and the MED effects n. It was found that raising x increases the exergy efficiency ε and there exists an optimal t_m which maximizes the water production m_w and ε; the influences of n include ε increasing 0.012% and *COW* decreasing by 0.02∼0.03$ per effect added.

Acknowledgements

The authors gratefully acknowledge the support of the National Natural Science Foundation of China (Grant Nos. 50836005, 51076152) and the National Basic Research Program of China ("973" Program) (Grant No. 2010CB227301).

Appendix A. Heat-transfer coefficient correlations used in the MED models [26]

The correlations for the overall heat transfer coefficient in various units are given by the following expressions:

$$U_e = 1.9394 + 1.40562 \times 10^{-3}\, T_i - 2.07525 \times 10^{-5}\, T_i^2 + 2.3186 \times 10^{-6}\, T_i^3$$

$$U_c = 1.6175 + 1.537 \times 10^{-4}\, T_v + 1.825 \times 10^{-4}\, T_v^2 - 8.026 \times 10^{-8}\, T_v^3$$

$$U_{PHE} = 14.18251642 + 1.1383865 \times 10^{-2}\, T_{cn} + 1.3381501 \times 10^{-2}\, T_{cw}$$

where U_e, U_c, and U_{PHE} are the overall heat transfer coefficient in the evaporator, condenser, and feed/distillate product preheater, all are in kW/m^2 °C, T_i is the brine boiling temperature in effect i, T_v is the vapor saturation temperature in the condenser, T_{cn} is the distillate condensate temperature entering the feed/distillate product preheater, and T_{cw} is the intake seawater temperature. All temperatures in the above correlations are in °C.

References

[1] Abdallaha H, Facchinib B, Danesc F, De Ruyckd J. Exergetic optimization of intercooled reheat chemically recuperated gas turbine. Energy Conversion and Management 1999;40:1679–86.
[2] Kesser KF, Hoffman MA, Baughn JW. Analysis of a basic chemically recuperated gas turbine power plant. Journal of Engineering Gas Turbine Power 1994;116:277–84.
[3] Harvey S, Kane ND. Analysis of a reheat gas turbine cycle with chemical recuperation using Aspen. Energy Conversion and Management 1997;38:1671–9.
[4] Hongguang Jin, Hui Hong, Ruixian Cai. A chemically intercooled gas turbine cycle for recovery of low-temperature thermal energy. Energy 2006;31:1554–66.
[5] Cocco D, Tola V, Cau G. Performance evaluation of chemically recuperated gas turbine (CRGT) power plants fuelled by di-methyl-ether (DME). Energy 2006;31:1446–58.
[6] Han W, Jin H, Zhang N, Zhang X. Cascade utilization of chemical energy of natural gas in an improved CRGT cycle. Energy 2007;32:306–13.
[7] Abdallah H, Harvey S. Thermodynamic analysis of chemically recuperated gas turbines. International Journal of Thermal Sciences 2001;40:372–84.
[8] Nakagaki T, Ogawa T, Hirata H, Kawamoto K, Ohashi Y, Tanaka k. Development of chemically recuperated micro gas turbine. Journal of Engineering Gas Turbine Power 2003;125:391–7.
[9] Hongguang Jin, Hui Hong, Baoqun Wang. A new principle of synthetic cascade utilization of chemical energy and physical energy. Science in China Ser. E. Engineering & Materials Science 2005;48:163–79.
[10] Zhang N, Lior N. Two novel oxy-fuel power cycles integrated with natural gas reforming and CO_2 capture. Energy 2008;33:340–51.
[11] Jonssona M, Yan J. Humidified gas turbines-a review of proposed and implemented cycles. Energy 2005;18:615–25.
[12] Darwisha MA, Al-Najema NM, Lior N. Towards sustainable seawater desalting in the Gulf area. Desalination 2009;235:58–87.
[13] Wang YQ, Lior N. Performance analysis of combined humidified gas turbine power generation and multi-effect thermal vapor compression desalination systems-Part 1: the desalination unit and its combination with a steam-injected gas turbine power system. Desalination 2006;196:84–104.
[14] Hisham TE, Hisham ME, Faisal M. Performance of parallel feed multiple effect evaporation system for seawater desalination. Applied Thermal Engineering 2000;20:1679–706.
[15] Darwish MA, Al-Asfour F, Al -Najem N. Energy consumption in equivalent work by different desalting methods: case study for Kuwait. Desalination 2003;152:83–92.
[16] Alasfour FN, Darwish MA, Bin Amer AO. Thermal analysis of ME-TVC+MEE desalination systems. Desalination 2005;174:39–61.
[17] Al-Najem NM, Darwish MA, Youssef FA. Thermovapor compression desalters: energy and availability-Analysis of single- and multi-effect systems. Desalination 1997;110:223–38.
[18] Ji MK, Utomo T, Woo JS, Lee YH, Jeong HM, Chung HS. CFD investigation on the flow structure inside thermo vapor compressor. Energy 2010;35:2694–702.
[19] Hamed OA, Zamamiri AM, Aly S, Lior N. Thermal performance and exergy analysis of a thermal vapor compression desalination system. Energy Conversion and Management 1996;37:379–87.
[20] Thibaut Rensonnet, Javier Uche, Luis Serra. Simulation and thermoeconomic analysis of different configurations of gas turbine (GT)-based dual-purpose power and desalination plants (DPPDP) and hybrid plants (HP). Energy 2007;32:1012–23.
[21] Choi HS, Kim YG, Song SL. Performance improvement of multiple-effect distiller with thermal vapor compression system by exergy analysis. Desalination 2005;182:239–49.
[22] Hoseyn Sayyaadi, Arash Saffari. Thermoeconomic optimization of multi effect distillation desalination systems. Applied Energy 2010;87:1122–33.
[23] Kambiz Ansari, Hoseyn Sayyaadi, Majid Amidpour. Thermoeconomic optimization of a hybrid pressurized water reactor (PWR) power plant coupled to a multi effect distillation desalination system with thermo-vapor compressor (MED-TVC). Energy 2010;35:1981–96.
[24] Fiorini P, Sciubba E. Modular simulation and thermoeconomic analysis of a multi-effect distillation desalination plant. Energy 2007;32:459–66.
[25] Aspen Plus®. version 11.1. Aspen Technology, Inc., http://www.aspentech.com/; 2010. 9.30.
[26] El-Dessouky HT, Ettouney HM, Al-Juwayhel F. Multiple effect evaporation-vapour compression desalination processes. Chemical Engineering Research and Design 2000;78:662–76.
[27] Kronenberg G, Lokiec F. Low-temperature distillation processes in single- and dual-purpose plants. Desalination 2001;136:189–97.
[28] Alhazmy Majed M. Feed water cooler to increase evaporation range in MSF plants. Energy 2009;34:7–13.
[29] Darwish MA, El-Dessouky H. The heat recovery thermal vapor-compression desalting system: a comparison with other thermal desalination processes. Applied Thermal Engineering 1996;16:523–37.
[30] Hamed Osman A, Al-Washmi Hamed A, Al-Otaibi Holayil A. Thermoeconomic analysis of a power/water cogeneration plant. Energy 2006;3:2699–709.

[31] Agashichev Sergei P, El-Nashar Ali M. Systemic approach for techno-economic evaluation of triple hybrid (RO, MSF and power generation) scheme including accounting of CO_2 emission. Energy 2005;30:1283–303.
[32] Gas turbine world 2010 handbook. Pequot Publishing, Inc; 2010.
[33] Lozza G, Chiesa P. Natural gas decarbonization to reduce CO_2 emission from combined cycles – Part I: partial oxidation. Journal of Engineering of Gas Turbines and Power 2002;124:82–8.
[34] Chiesa Paolo, Consonni Stefano. Natural gas fired combined cycles with low CO_2 emissions. Journal of Engineering of Gas Turbines and Power 2000;122:429–36.
[35] Alessandro Corrandetti, Umferto Desideri. Analysis of gas-steam combined cycles with natural gas reforming and CO_2 capture. Journal of Engineering of Gas Turbines and Power 2005;127:545–52.
[36] U.S. Energy Information Administration. Natural gas weekly update, http://www.eia.doe.gov/oog/info/ngw/ngupdate.asp; 2010. 9.30.
[37] U.S. Energy Information Administration. Average Retail Price of Electricity to Ultimate Customers by End-Use Sector, by State, http://www.eia.doe.gov/electricity/epm/table5_6_a.html; 2010. 9.30.
[38] News CBS. Water prices rising, worldwide, http://findarticles.com/p/articles/mi_m1272/is_2743_135/ai_n19039009/; 2010. 9.30.
[39] Larson ED, Ren T. Synthetic fuel production by indirect coal liquefaction. Energy for Sustainable Development; 2003. VII(4).
[40] Kreutz T, Williams R, Consonni S, Paolo Chiesa. Co-production of hydrogen, electricity andCO_2 from coal with commercially ready technology Part B: economic analysis. International Journal of Hydrogen Energy 2005;30:769–84.
[41] Stoll RE, Linde von F. Hydrogen-what are the costs. Hydrocarbon Processing 2002;79:42–6.
[42] Liu M, Lior N, Zhang N, Han W. Thermoeconomic analysis of a novel zero-CO_2-emission high-efficiency power cycle using LNG coldness. Energy Conversion and Management 2009;50:2768–81.
[43] Zhang N, Lior N, Liu M, Han W. COOLCEP (cool clean efficient power): a novel CO_2-capturing oxy-fuel power system with LNG (liquefied natural gas) coldness energy utilization original research article. Energy 2010;35:1200–10.